Supplemental Material: "He-McKellar-Wilkens topological phase in atom interferometry"

Steven Lepoutre, Alexandre Gauguet, Gérard Trénec, Matthias Büchner, Jacques Vigué

Supplemental Material: "He-McKellar-Wilkens topological phase in atom interferometry"

S. Lepoutre, A. Gauguet, G. Trénec, M. Büchner, and J. Vigué

Laboratoire Collisions Agrégats Réactivité-IRSAMC
Université de Toulouse-UPS and CNRS UMR 5589, Toulouse, France
e-mail: jacques.vigue@irsamc.ups-tlse.fr
(Dated: September 7, 2012)

We provide here additional details concerning several points briefly discussed in the letter. In particular, we give more details concerning the experimental setup, its defects and the stray phase shifts induced by these defects. We also give an overview of the analysis of these stray phase shifts.

PACS numbers: 03.65.Vf; 03.75.Dg; 39.20.+q

I. AC-HMW CONNECTION

The Aharonov-Casher [1] phase and the He-McKellar [2] and Wilkens [3] phase are connected by electric-magnetic duality, as illustrated in figure 1. It is impossible to detect the He-McKellar-Wilkens (HMW) phase with such a scheme because magnetic monopoles are hypothetical particles [4]. The experiments proposed by Wilkens [3], by Wei *et al.* [5] and by Sato and Packard [6] do not involve magnetic monopoles but the propagation of polarizable atoms (or molecules) in magnetic fields, the electric dipole being induced by an electric field perpendicular to the magnetic field. The question whether such an experiment is a test of the He-McKellar-Wilkens idea is worth discussing. In our opinion, the important point is that an electric dipole $\mathbf{d}$ propagates in a magnetic field $\mathbf{B}$ perpendicular to $\mathbf{d}$ and to the atom velocity $\mathbf{v}$. Magnetic monopoles would produce a diverging magnetic field, leading to a non-zero HMW phase $\varphi_{HMW} = \oint (\mathbf{d} \times \mathbf{B}) \cdot \mathbf{v} dt/\hbar$ but the exact nature of the magnetic field source is irrelevant and any field configuration which yields a non vanishing HMW phase is a test of the HMW effect. The idea of Wilkens [3] is to use the same dipole direction on the two interferometer arms but different magnetic fields thanks to ferromagnetic material. Wei *et al.* [5] go one step further and propose to have states with opposite induced dipoles in a common homogeneous magnetic field. We may note that similar aspects were discussed for the Aharonov-Casher phase [7, 8].

II. THE EXPERIMENTAL SETUP

In this section, we give further details about the interaction region used for the observation of the HMW phase: this interaction region is schematically represented in figure 1 of our letter.

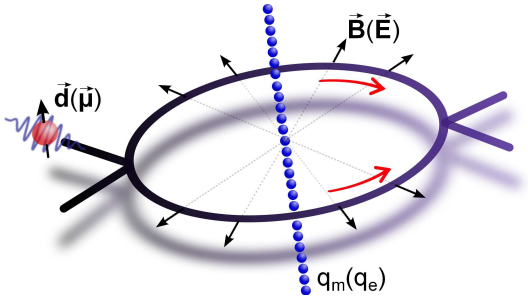

FIG. 1: Electric-magnetic duality connection between the Aharonov-Casher and He-McKellar-Wilkens phases (following [9]). The interferometer arms encircle a line of charges: for the He-McKellar-Wilkens phase, the electric dipole $\mathbf{d}$ interacts with the magnetic field $\mathbf{B}$ created by a line of magnetic monopoles q_m, while, for the Aharonov-Casher phase, the magnetic dipole $\boldsymbol{\mu}(F, m_F)$ interacts with the electric field $\mathbf{E}$ created by a line of electric charges q_e.

A. The electric fields

The electric fields $\mathbf{E}$ are produced by two plane capacitors sharing a thin "septum" electrode [10]; the electrodes are in vertical planes so that the electric field is horizontal, along the x-axis. The septum is a 20 μm-thick aluminium foil, with a surface roughness better than 2 μm while the other electrodes are 5 mm-thick polished glass plates with an aluminium coating. Along the z-direction, two 5 mm-long guard electrodes surround a 48 mm-long high-voltage electrode, with 1 mm-wide gaps between high-voltage and guard electrodes. The capacitors are assembled by gluing together the electrodes and 1.1 mm-thick glass spacers. A specific procedure was used to glue the septum in order to keep it stretched even when the temperature rises [11]. The electric fields produced by each capacitor was investigated using polarizability phase shift measurements and by calculations [12]. Except near the guard electrodes, the electric field is homogeneous, with a modulus $E(\mathrm{kV/m}) \approx 0.9V$, where V is the applied voltage in Volts. V can be positive or negative, in order to test the effect of field reversals.

When measuring the HMW phase shift, we equalize the polarizability phase shifts induced on the two interferometer arms by tuning the ratio of the voltages applied on the two capacitors with potentiometers, using a common power supply. In this way, the residual Stark phase shift is small, near 0.1 rad.

B. Magnetic field

The magnetic field **B** is designed to be vertical, along the y-axis, and homogeneous. It is produced by two rectangular coils in the (x,z) plane. These coils, which surround the capacitors, are located $\sim$ 5 mm above and below the capacitor mid-plane. Each coil is made of 2 layers of 7 turns of 1.5 mm-diameter enameled copper wire coiled on a common water cooled brass support. The support dimensions are 83×18 mm^2. The two coils are connected in series. Thermal conduction is ensured by a high thermal conductivity glue (Stycast 2850 FT) and the coil temperature rises by about 10 K for a 20W Joule power, corresponding to a current $I = 26$ A, if applied 50% of the time as in most experiments. We have measured the magnetic field with a 3D Hall probe and found it in agreement with its calculated dependence. Over the region where the electric field is applied, the magnetic field is quasi-vertical and its value varies by less than 4%. At the coil center of symmetry, the field is given by $B/I \approx 5.6 \times 10^{-4}$ T/A, so that $B_{max} = 14.6$ mT. The current I can also be positive or negative, in order to test the effect of field reversals.

The field homogeneity is not perfect and the small magnetic field gradient, which exists in the x-direction, induces Zeeman phase shifts. From the measured shifts, we deduce that the magnetic field difference between the two interferometer arms is about $\delta B/B \sim 10^{-4}$: this small difference is expected if the distance along the x-axis between the septum and the coil symmetry plane is about 200 μm, well within the defects of our construction. In order to cancel the Zeeman phase shifts, we have introduced a compensation coil which produces a magnetic field gradient between the two interferometer arms at another place so that the total magnetic phase shift vanishes. This compensation coil, located at mid-distance between the first and second laser standing waves, is made of 9 turns of 1.5 mm-diameter copper wire on a 30 mm-diameter support. The coil axis is horizontal, along the x-axis and the coil center is at about 10 mm from the interferometer arms. It creates a magnetic field gradient in the x-direction. This coil is cooled by thermal conduction through its support and temperature rise limits the compensation current I_c to 5 A, corresponding to a maximum field seen by the atoms near 2×10^{-3} T.

III. MEASUREMENT PROCEDURE AND DATA SET

The detection of the HMW effect requires a measurement procedure which is not sensitive to the phase drift of the interferometer. This procedure is briefly described in our letter: it consists in alternating several configurations of the electric field E and the magnetic field B during a fringe sweep. We carefully checked that it does not induce any unwanted bias. In a first step, we have characterized our setup by recording fringes with only one field applied, sweeping a large range of V, I and I_c values. Then, to measure the HMW phase shift, we recorded data for a set of (V, I) values represented in figure 2. Our first measurements were done with a 4-field procedure: during a fringe scan, the following values of (V, I) alternate $((0,0)$, $(V,0)$, (V,I), $(0,I))$ as in figure 2 of our letter. We then modified this procedure to use a 6-field procedure $((0,0)$, $(+|V|,0)$, $(+|V|,I)$, $(0,I)$, $(-|V|,I)$, $(-|V|,0))$ and most of the data was recorded in this way. The advantage of the 6-field procedure is to give more direct measurements of the effects of electric field reversals. To avoid high transient voltages associated to reversal of the coil currents, we have studied the effect of magnetic field reversal by recording successively data with same V value and opposite I values. We deduce from these measurements the value of $\varphi_{EB}(V, I)$ given by equation (4) of our letter but also $\varphi_E(V)$ and $\varphi_B(I)$. We also get very accurate values of the relative visibility $\mathcal{V}_r(V, I) = \mathcal{V}(V, I)/\mathcal{V}(0, 0)$ as well as $\mathcal{V}_r(V) = \mathcal{V}(V)/\mathcal{V}(0)$ and $\mathcal{V}_r(I) = \mathcal{V}(I)/\mathcal{V}(0)$. All this information is used in the analysis of systematic effects due to small defects of our setup.

As $\varphi_{HMW} \propto VI$ and as its expected value is small, we have collected data with moderate to large values of the VI product and this is why we have no data with $|VI| < 4000$ V.A. This choice was not optimum because systematic effects increase rapidly with the magnetic field and the data with $|I| > 12$ A has been discarded from the final analysis. Nevertheless, the data collected with large values of $|I|$ has given very useful information on systematic effects.

IV. THEORY OF THE SIGNAL: PREDICTION OF SYSTEMATIC EFFECTS ON THE FRINGE PHASE AND VISIBILITY

Here we discuss the various phase shifts induced by the electric and magnetic field on the atom interferometer fringes and, for each phase shift, the origin of its dispersion. We then explain how these dispersions induce stray phase shifts and the way we evaluate these effects.

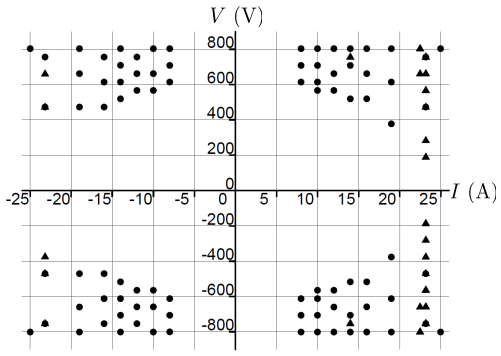

FIG. 2: Data set collected for the measurement of the HMW phase in the (I, V) plane: a triangle for a 4-field procedure or a bullet for a 6-field procedure.

A. Origins of the various phase shifts

Any perturbation term U added to the atom Hamiltonian modifies the propagation phase of the atom. The fringe phase shift in an atom interferometer is given by:

$$\varphi_{dyn} = -\oint \frac{U(\mathbf{r})\,dt}{\hbar} = -\oint \frac{U ds}{\hbar v} \tag{1}$$

where $\mathbf{r}$ is the atom position and the integral follows the unperturbed interferometer arms. In the second form, ds is the curvilinear element of the interferometer arms and v the atom velocity. This first order expression is valid if U is small enough with respect to the atom kinetic energy [13]. In our experiment, $U = U_Z(F, m_F) + U_S$, respectively the Zeeman and the Stark term. The associated dynamic phase shifts are the Stark (or polarizability) phase shift φ_S and the Zeeman phase shift $\varphi_Z(F, m_F)$. Equation (1) is valid as long as the applied fields are small enough, which is the case in our experiment. We must also add the topological phase shifts φ_{AC} and φ_{HMW} respectively due to the Aharonov-Casher and He-McKellar-Wilkens effects to get the total fringe phase φ:

$$\begin{aligned} \varphi \;=\; & \varphi_d + \varphi_S + \varphi_Z(F, m_F) \\ & + \varphi_{AC}(F, m_F) + \varphi_{HMW} \end{aligned} \tag{2}$$

where φ_d is the diffraction phase, which is used to scan the fringes.

The Stark term is $U_S = -2\pi\varepsilon_0\alpha\mathbf{E}^2$. With our maximum field $E \approx 770$ kV/m ($V \approx 850$ V), the Stark phase shift induced on each arm exceeds 300 rad. Thanks to a fine tuning of the ratio of the voltages applied to the two capacitors, the resulting Stark phase shift is small $\varphi_S \sim 0.1$ rad.

With the rather large magnetic field applied in the HMW interaction region, hyperfine uncoupling occurs so that we must include the hyperfine Hamiltonian and the Zeeman Hamiltonian in the perturbation term $U_Z(F, m_F)$. As in previous studies [14–16], we assume an adiabatic behavior: the magnetic field $\mathbf{B}$ direction is slowly varying in space so that the projection m_F of the $\mathbf{F}$ angular momentum on an axis parallel to the local magnetic field $\mathbf{B}$ is constant. If we assume that the interferometer arms are very close to the z-axis and if $\delta x(z)$ is the distance between the two arms, the Zeeman phase shift is given by:

$$\varphi_Z(F, m_F) = -\int \frac{\partial U_Z(F, m_F)}{\partial B}\frac{\partial B}{\partial x}\frac{\delta x(z)\,dz}{\hbar v} \tag{3}$$

Because of hyperfine uncoupling, the Zeeman energy shift and the Zeeman phase shift are complicated functions of F, m_F and of the HMW coil current I. Although the relative field difference between the two interferometer arms is small, $\delta B/B \sim 10^{-4}$, the resulting phase shift is large, up to $\varphi_Z(F = 2, m_F = \pm 2) \approx \pm 11$ rad for $B = 14$ mT. Because the Zeeman phase shift strongly depends of F and m_F and because the atoms are distributed over the 8 ground state sub-levels, the fringe visibility becomes rapidly very small when the magnetic field increases [14–16]: for instance, the visibility vanishes when $I \approx 6$ A. We compensate this Zeeman phase shift with the additional gradient produced by the compensation coil and we have found that compensation is obtained with $I_c \approx |I|/3$. However, the compensation coil produces a low field which can compensate only the linear part of the Zeeman phase shift. As shown in figure 3, this compensation is very efficient, with the relative fringe visibility being larger than 70% up to a current $|I| = 12$ A. When the HMW coil current is large, $|I| > 15$A, the compensator current was fixed $I_c = 5$ A. The relative fringe visibility vanishes for $|I| \approx 18$ A and presents a revival with a phase shift close to π for $I = 23$ A and a relative visibility near 70% (this revival is explained in [11]).

The HMW phase shift is given by equation (2) of our letter and its maximum value is $\varphi_{HMW} \approx 27$ mrad.

The AC phase shift [1] is given by:

$$\phi_{AC}(F, m_F) = -\oint \frac{[\mathbf{E}(\mathbf{r}) \times \boldsymbol{\mu}(F, m_F)] \cdot d\mathbf{r}}{\hbar c^2} \tag{4}$$

where $\boldsymbol{\mu}(F, m_F)$ is the magnetic moment of the F, m_F sub-level. The maximum value of the AC phase shift is $|\varphi_{AC}(F = 2, m_F = \pm 2)| \approx 70$ mrad. In the interpretation of the observed data, we will use the theoretical value of the AC phase shift.

In equation 3, we have not included the Berry's phase [17] due to the fact that the direction of the magnetic field is not constant over the interferometer arms. The measured Berry's phase is the difference of the Berry's phases over the two interferometer arms and this difference is expected to be very small because the magnetic field homogeneity is very good: from the Zeeman phase shifts, we estimate that the relative difference of magnetic field $\delta B/B$ is $\delta B/B \approx 10^{-4}$ for the HMW coil and $\delta B/B \approx 10^{-3}$ for the compensating coil. Moreover, the measured Berry's phase should not be sensitive to the

presence of the electric field, because the Stark term is the same for all the hyperfine sub-levels with an excellent accuracy [12] and, as a consequence, the measured Berry's phase should have the same value in $\varphi_{E+B}(V, I)$ and in $\varphi_B(I)$ so that it should be fully canceled in $\varphi_{EB}(V, I)$.

A more complex Berry's phase involving the electric and magnetic fields was detected in the measurement of the electron dipole moment [18]. This Berry's phase is proportional to the solid angle of the spatial circuit of the magnetic field directio, where the magnetic field is the one seen by the atom in its rest frame (this means that it includes the motional magnetic field due to the electric field). This Berry's phase is an edge effect, which is sensitive to the difference of transverse components of the magnetic fields at the two ends of the electric field region. As it involves the motional magnetic field due to the electric field, this effect is related to the AC phase (but the AC phase, which is proportional to the electric field and to the length of the path in the field, is not an edge effect). We have put figures in the formula of reference [18] and the effect is completely negligible in our experiment: this can be explained by the fact that we use larger magnetic fields and lower electric fields.

B. Dispersion of the phase shifts

A dispersion of the fringe phase reduces the fringe visibility and, as shown below, it may also induce systematic errors on the phase measurements.

The Stark and Zeeman phase shifts are the only phases which depend on the atom velocity: equation (1) proves that $\varphi_S \propto 1/v$ and equation (3) proves that $\varphi_Z(F, m_F) \propto 1/v^2$ because $\delta x(z)$ is proportional to $1/v$. The atomic beam velocity distribution is given by [12]:

$$P(v) = \frac{S_\parallel}{u\sqrt{\pi}} \exp\left[-\left((v-u)S_\parallel/u\right)^2\right] \qquad (5)$$

where u is the mean velocity and $S_\parallel$ is the parallel speed ratio. During the HMW measurements, the associated phase dispersion is not very large because the velocity distribution is narrow (with $S_\parallel \approx 7$ corresponding to a half-width at half maximum close to 10% of the mean velocity) and because the phase shifts are small: the largest phase shift is the Zeeman phase shift close to π near the fringe visibility revival with $I \approx 23$ A. When the phase dispersion is small, it is possible to use analytic results to calculate the effects of the phase dispersion on the fringe phase and visibility: this calculation is described for the Stark phase shift in ref. [12] and for the Zeeman phase shift in [19] and it can be easily generalized to the case where the two phase shifts are simultaneously present.

The main source of phase dispersion comes from the fact that the signal is an average over different atom trajectories. Atom diffraction is based on the transfer of momentum from the laser standing wave to the atom. The laser beams being horizontal, the direct and diffracted beams are in the same horizontal plane, so that the interferometer signal measures the propagation phase difference on the two arms at the same altitude y. This phase difference is a function of the y-coordinate because of the applied fields are not perfectly independent of y. The electric field of a given capacitor is inversely proportional to the capacitor spacing and if the spacings of the two capacitors are different functions of y, the Stark phase shift is function of y. In the interaction region, the magnetic field gradient $\partial B/\partial x$ is a function of the altitude y; this function goes through a minimum for the y-value corresponding to the mid-distance between the two HMW coils but the interferometer arms are not well centered with respect to the HMW coils and field calculations show that $\partial B/\partial x$ can vary by up to 10% along the estimated height of the atomic beam. Finally, the diffraction phase φ_d is also a function of y because the laser standing wave mirrors M_i are not perfectly vertical (this effect is analyzed in ref. [20]). We have also considered the possible effects of contact potentials on the electric fields, i.e. spatial variations of the order of 100 mV of the electrode work function, but this effect appeared to be fully negligible in our experiment.

Finally, the Zeeman phase shift is a function of the F, m_F sub-level. If we neglect the nuclear contribution to the Zeeman energy shift (this is a very good approximation), the 8 sub-levels form 4 pairs of levels with opposite Zeeman energy shifts: one pair is formed of the $F = 2$ $m_F = \pm 2$ sub-levels and the three other pairs are formed of the levels having the same m_F value. If the two levels inside each pairs give equal contributions to the detected signal, the measured Zeeman phase shift φ_B vanishes [14, 16]. During the HMW measurements, these contributions were close to such a perfect balance (this question is discussed below): φ_B was always small, and its value is a sensitive test of the relative weights of the (F, m_F) sub-levels.

C. Effects of a phase shift dispersion

In this part, we study the consequence of a phase dispersion on the phase shift measurement and we consider only the phases φ_d, φ_S and φ_Z, because the phases φ_{HMW} and φ_{AC} are so small that their dispersion cannot play a significant role. Two types of dispersions are taken into account in our analysis: the position distribution due to the y-distribution of intensity of the atomic beam and the distribution over the (F, m_F) sub-level. These dispersions modify the fringe visibility but also lead to systematic effects on the measured phase shift.

Let us first consider the case of the dispersion of the phase shift $\varphi(y)$ with the y-coordinate. The atomic beam has a non-negligible size along the y-direction and we note $P(y)$ the distribution of the atomic beam intensity along this coordinate, with $\int dy P(y) = 1$. The fringe signal for one sub-level is given by the following average:

$$I = I_0 \int dy P(y) \left[1 + \mathcal{V}_0 \cos\left(\varphi(y)\right)\right] \quad (6)$$

The average over y with the weight $P(y)$ is noted $\langle ... \rangle$ and we define $\delta\varphi = \varphi(y) - \langle\varphi\rangle$. If we expand the equation (6) up to the third order in $\delta\varphi$, we get the modified visibility $\mathcal{V}_m$ and the modified phase shift φ_m given by:

$$\begin{aligned} \frac{\mathcal{V}_m}{\mathcal{V}_0} &= 1 - \frac{\langle\delta\varphi^2\rangle}{2} \\ \varphi_m &= \langle\varphi\rangle - \frac{\langle\delta\varphi^3\rangle}{6} \end{aligned} \quad (7)$$

The relative visibility $\mathcal{V}_m/\mathcal{V}_0$ reveals the dependence of the Stark and Zeeman phase shifts with the atom trajectory altitude y. In particular, when two perturbations a and b producing the phase shifts φ_a and φ_b are simultaneously present, the modified visibility $\mathcal{V}_m$ and the modified phase shift φ_m cannot be deduced from the knowledge of the same quantities when the two perturbations are acting separately: this is due to the cross terms $\langle\delta\varphi_a\delta\varphi_b\rangle$, present in $\mathcal{V}_m$, and $\left\langle (\delta\varphi_a)^2 \delta\varphi_b \right\rangle$ and $\left\langle \delta\varphi_a \left(\delta\varphi_b\right)^2 \right\rangle$, present in φ_m.

Besides the y-position distribution, we must sum the signals of the 8 (F, m_F) sub-levels. As the Zeeman phase shifts may be important, an expansion in powers of $\delta\varphi_Z\left(F, m_F\right)$ would not be a good approximation and, using equation (7), we must evaluate the sum:

$$I = \sum_{F,m_F} I_{F,m_F} \left[1 + \mathcal{V}_{F,m_F} \cos\left(\langle\varphi_{F,m_F}\rangle - \frac{\langle\delta\varphi^3_{F,m_F}\rangle}{6}\right)\right] \quad (8)$$

The intensities I_{F,m_F} are normalized, $\sum_{F,m_F} I_{F,m_F} = 1$ and their values are discussed below. The visibility $\mathcal{V}_{F,m_F}$ and the phase $\langle\varphi_{F,m_F}\rangle - \langle\delta\varphi^3_{F,m_F}\rangle/6$ of the contribution of the (F, m_F) sub-level to the signal are functions of F, m_F. From this calculation, we deduce the modified fringe visibility $\mathcal{V}_m$ and the fringe phase shift φ_m for the complete signal and we define a complex reduced visibility:

$$\underline{\mathcal{V}}_r = \mathcal{V}_m \exp\left(i\varphi_m\right)/\mathcal{V}_0 \quad (9)$$

which is used in figure 3. For instance, equation 7 proves that the value of $\mathcal{V}_{F,m_F}$ for a given F, m_F sub-level is different in the presence or absence of the electric field, and the modifications are opposite inside a pair of levels with opposite Zeeman energy shifts. This is an important source of systematic effects. We have developed these calculations to analyze all the systematic phase shifts which may appear in our measurement of the HMW phase. Their volume exceeds what can be described in this supplemental material. As a consequence we will present only some tests of these results.

D. Intensities of the F, m_F sub-levels

The 8 (F, m_F) sub-levels are equally populated in the incoming atomic beam: we have taken care to prevent any strong magnetic field gradient which could deviate in a different way these sub-levels so that, for the incoming atomic beam, $I_{F,m_F} = 1/8$. However, the diffraction amplitudes depend on the hyperfine quantum number F, because the laser frequency detuning $\delta_L\left(F\right)$ is different for these two levels because of the ground state hyperfine splitting [21]. The interferometer transmission is thus a function of F but it is independent of m_F: it can be described by parameter measuring the population imbalance. For a given laser power density in the standing waves, there is a value of the laser detuning which equalizes the interferometer transmissions for the two hyperfine levels and we have taken care to work near these optimum conditions. The measured Zeeman phase shift, which vanishes if these transmissions are equal, gives a sensitive test of the transmission ratio. We estimate that, in our measurements of the HMW phase, the intensities I_{F,m_F} deviate from their optimum value $1/8 = 12.5\%$ by not more that $\pm 1.5\%$ and this deviation is quasi-random, with a negligible average value.

An important consequence of the quasi-equal population of the 8 (F, m_F) sub-levels concerns the AC phase shift. In each pair of F, m_F sub-levels with opposite Zeeman energy shifts, the sub-levels have opposite magnetic moments and they have accordingly opposite AC phase shifts. The existence of the AC phase shifts induces only a very small shift of the measured phase; this shift does not vanish only because, following equation (7), the contributions of the two levels have not the same visibility. The presence of the AC phase shift substantially modifies the measured fringe visibility as shown below in figure 5.

E. Concluding remarks

In this part, we have given an overview of the way we developed a detailed description of the signal of our atom interferometer. This detailed description, which is quite complex, will be published elsewhere. The interest of this analysis is that it gives an understanding of most of the defects of our interferometer and it predicts the variations of the fringe visibility and the existence of systematic phase shifts due to cross effects appearing when the electric and magnetic fields are simultaneously applied. We are going to test some predictions of this model in the next section.

V. SOME TESTS OF SYSTEMATIC EFFECTS

We first present here some results obtained with the application of either the magnetic field or the electric field. In a next step, we will discuss results involving the simultaneous application of both fields.

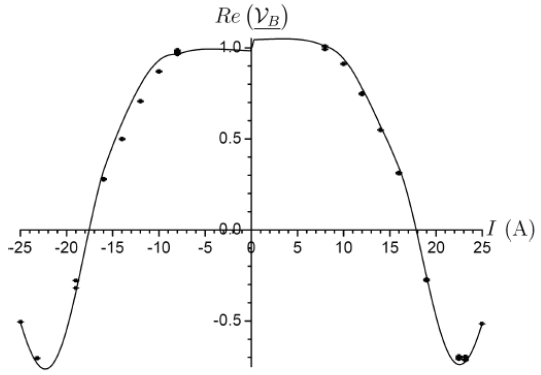

FIG. 3: Real part of the complex relative visibility $\underline{\mathcal{V}}_r$ defined by equation 9 as a function of the current I in the HMW coil. The current I_c in the compensating coil being equal to $I_c \approx |I|/3$ when $|I| < 15$ A and to $I_C = 5$ A when $|I| > 15$ A. The points are measured data and the curve is the result of our analytic model fitted on a very large data set.

A. Magnetic field only

We have developed analytic expressions to represent the Zeeman phase shifts $\varphi_Z(F, m_F)$ as a function of F, m_F and of the currents I in the HMW coil and I_C in the compensator. The compensator field is always weak enough and the phase shifts are well described by linear Zeeman effect i.e. $\varphi_Z(F, m_F) \propto |I_c|$ (the independence with the sign of the current is due to adiabatic following) and only one parameter must be fitted on the experimental data to describe these phase shifts. The HMW coils produce a considerably larger magnetic field which induces hyperfine uncoupling. In order to describe the variations of $\varphi_Z(F, m_F)$ with the current $|I|$, we have expressed $\varphi_Z(F, m_F)$ by a power expansion in $|I|$ up to the third order, so that 3 parameters must be fitted on experimental data to describe all the Zeeman phase shifts. However, the accuracy of this expansion decreases at large fields, the relative deviations being equal to 3% for the $m_F = \pm 1$ sub-levels and 12% for the $m_F = 0$ sub-levels with the strongest magnetic field $B = 1.4 \times 10^{-2}$ T. This lack of accuracy is the main weakness of our model. A supplementary refinement was needed to take into account the weak inhomogeneity of the laboratory field, i.e. the field when $I = I_c = 0$ (this refinement requires the introduction of 3 additional parameters). This field is weak enough to yield linear Zeeman phase shifts and its presence slightly breaks the parity of $\varphi_Z(F, m_F)$ with regards to I or I_c and it induces a quasi-discontinuity near $I = I_c = 0$ (see figure 3).

Finally, the analytic expressions describing the variations of $\varphi_Z(F, m_F)$ with I and I_C have been fitted on a very large data set involving 150 measurements using the HMW coils, the compensation coil, or both acting simultaneously. This fit involved 9 parameters: 7 parameters related to the magnetic field, the parallel speed ratio $S_\parallel$ describing the atomic beam velocity distribution and one extra parameter describing the population imbalance between the $F = 1$ and $F = 2$ levels: the 8 parameters are fitted with a single value for all the experimental data points while the population imbalance parameter must be separately fitted for different series of experiments as it varies with the laser frequency detuning. We cannot describe these results in detail but the fitted values of most parameters are very well defined with error bars of the order of a few percent. We present in figure 3 the visibility as a function of the current I in the HMW coils, with the compensator in operation. The good agreement between our model and the measured data proves that our model describes well the Zeeman phase shifts.

B. Electric field only

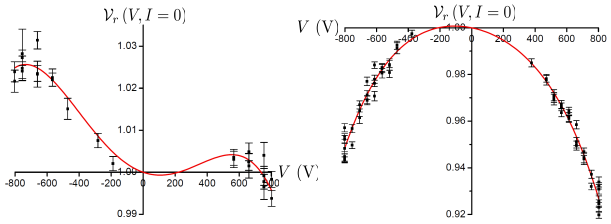

FIG. 4: Relative visibility $\mathcal{V}_r(V, I = 0)$ as a function of the applied voltage V, for two series of measurements performed with different adjustment of the mirrors of the laser standing waves. In both cases, the full (red) line represents the fit of the data which is described in the text.

We will not discuss the experiments done with a voltage applied to one capacitor only: these experiments have been used to characterize the capacitors and the atomic beam velocity distribution. We discuss here only the measurements performed with almost the same Stark phase shift on both arms so that the measured Stark phase shifts is small, $\varphi_S \approx 0.1$ rad. We have not found very interesting results when studying φ_S itself: if the temperature is not fully stabilized during the experiment, φ_S presents drifts because the temperatures of the two capacitors drift with different rates. On the contrary, the visibility gives important information on the y-dependence of the Stark phase shift φ_S and of the diffraction phase φ_d. We must also take into account the AC phase in the presence of the laboratory magnetic field. Figure 4 presents the relative visibility for two series of measurements performed with two different alignments of the standing wave mirrors i.e. with two different functions $\varphi_d(y)$. In all experiments, the relative visibility $\mathcal{V}_r(V) = \mathcal{V}_m(V)/\mathcal{V}_0$ is well described by a fourth order polynomial of V with a constant term equal to 1 and a null third order term, as predicted by our calculations. The fourth order coefficient is fairly independent of the mirror alignment and it simply measures the spatial dispersion of φ_S; the first order term is directly sensitive to the AC phase and the second order term is sensitive to

the correlation of the spatial dependences of $\delta\varphi_d(y)$ and of $\delta\varphi_S(y)$. We are going to discuss the effect of the AC phase on the visibility in the next section.

C. Concluding remarks

In this section, we have presented some tests of our model which describes the phase and the visibility of the interference fringes in the presence of an applied electric or magnetic field. The description of the Zeeman phase shifts is complicated by hyperfine uncoupling and by the inhomogeneity of the laboratory magnetic field when the currents in the HMW and compensator coils are both vanishing but the model works well and its accuracy is very good, except for the largest values of the magnetic field produced by the HMW coil. The main effect of the Zeeman interaction is to modify the fringe visibility and these modifications are very well explained by our model. The electric field induces the Stark and Aharonov-Casher phase shifts: the measured phase shifts are weak and sensitive to thermal distortions of the capacitors but the dispersion of these phase shifts, which is due to the capacitor defects on one hand and to the F, m_F-dependence of the Aharonov-Casher phase shift on the other hand, induces variations of the fringe visibility which are well described by our calculations.

VI. SIMULTANEOUS APPLICATION OF THE ELECTRIC AND MAGNETIC FIELDS

¿From the measured data, we get $\varphi_{EB}(V,I)$ defined by equation (4) of our letter and its counterpart for the relative visibility, $\mathcal{V}_{EB}(V,I) = [\mathcal{V}(V,I)\,\mathcal{V}(0,0)]\,/\,[\mathcal{V}(V,0)\,\mathcal{V}(0,I)]$. This quantity measures the non-additive character of the visibility modifications by the electric and magnetic perturbations. Our model predicts the variations with V and I of φ_{EB} and $\mathcal{V}_{EB}$: the various terms which appear in the model predictions can be easily sorted out by their parity with respect to V- or I-reversal. In order to compare the model prediction with experimental results, we isolate in the measured data the component which has a given parity with respect to V- or I-reversal: this is done by combining data for opposite values of V and/or of I and taking either the half difference or the average.

A. The V-odd part of the relative visibility, $\mathcal{V}_{EB}(V,I)$

We first illustrate the efficiency of our model by comparing the variations with the current I of the V-odd part of the visibility $\mathcal{V}_{EB}(V,I)$: this V-odd part is given by the difference $\Delta_V\mathcal{V}_{EB} = [\mathcal{V}_{EB}(V,I) - \mathcal{V}_{EB}(-V,I)]\,/2$. Our model predicts that this quantity is non-zero because of the AC phase and

$$\Delta_V\mathcal{V}_{EB} = -\frac{\sum_{m_F=-1}^{2}\varphi_{AC}(F=2,m_F)\sin\varphi_Z(F=2,m_F)}{\sum_{m_F=-1}^{2}\cos\varphi_Z(F=2,m_F)} \tag{10}$$

Figure 5 compares some measurements of $\Delta_V\mathcal{V}_{EB}$ to its calculated values following equation (10): the agreement is reasonably good, the more so as there is no fitted parameter. The model results are very sensitive to the Zeeman phase shifts and these measurements are a good qualitative test for the consistency of the calculated Zeeman phase shifts.

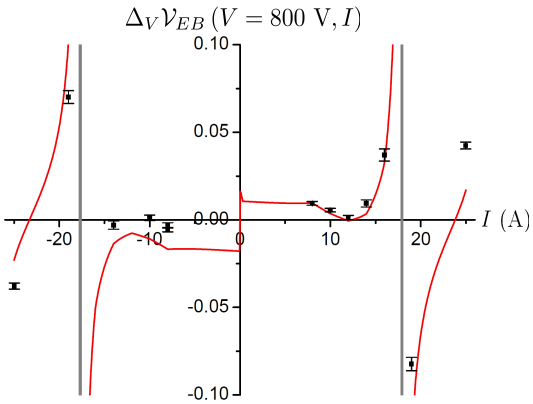

FIG. 5: $\Delta_V\mathcal{V}_{EB}(V,I)$ with $V = 800$ V is plotted as a function of the applied current I A in the HMW coil. The squares represent our measured values while the thin (red) line is the result of our model. The thick vertical (grey) lines indicate the I-values for which the visibility vanishes as a result of the dispersion of φ_Z with F, m_F. The modification of the visibility diverges for these values of the current I.

B. The V-even part of the phase shift $\varphi_{EB}(V,I)$

Our model predicts that the main systematic effects in $\varphi_{EB}(V,I)$ are even with respect to V- and I-reversals. We illustrate this term by considering the average $\mathcal{M}_V\varphi_{EB} = [\varphi_{EB}(V,I) + \varphi_{EB}(-V,I)]\,/2$: this quantity would vanish in the absence of defects, as φ_{HMW} is odd with respect to V- and I-reversals. Our model predicts that the dominant term in $\mathcal{M}_V\varphi_{EB}$ is given by:

$$\mathcal{M}_V\varphi_{EB} = -\frac{\sum_{m_F=-1}^{2}\langle\delta\varphi_S\delta\varphi_Z\rangle\sin\varphi_Z}{\sum_{m_F=-1}^{2}\cos\varphi_Z} \tag{11}$$

The $F = 2, m_F$ dependence of φ_Z and $\delta\varphi_Z$ being omitted for simplification. In figure 6, we compare some measurements of $\mathcal{M}_V\varphi_{EB}$ and the predictions of our model

in this case which also includes a smaller, higher-order term: thus two parameters have been fitted on the complete data set. Their values agree with expectations deduced from independent measurements or estimates of $\delta\varphi_S$ and $\delta\varphi_Z(F, m_F)$.

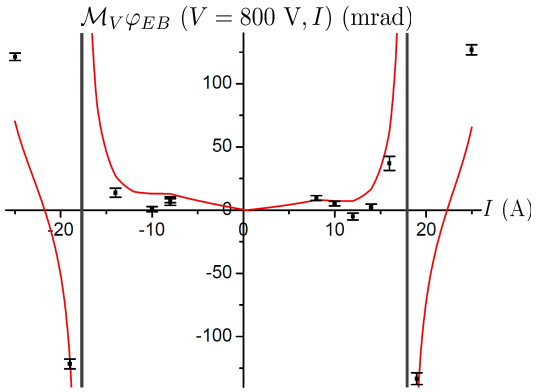

FIG. 6: Measured values of $\mathcal{M}_V\varphi_{EB}(V, I)$ as a function of I, with $V = 800$ V. The dots are the measured data and the curve is the result of our model. As in figure 5, thick vertical (grey) lines correspond to the cancelation of the visibility due to the dispersion of the magnetic phase shifts.

C. A stray phase shift which is not predicted by our model

This stray phase shift is odd with respect to V-reversal and even with respect to I-reversal. To extract this term, we first take the combination $\Delta_V\varphi_{EB}(V, I) = [\varphi_{EB}(V, I) - \varphi_{EB}(-V, I)]/2$ which is the odd with respect to V-reversal and we take the average for opposite I-values given by $\mathcal{M}_I(\Delta_V\varphi_{EB}) = [\Delta_V\varphi_{EB}(V, I) + \Delta_V\varphi_{EB}(V, -I)]/2$. The measured values of this quantity are plotted in figure 7 as a function of the voltage V for all the data points with the current I varying in the range from 5 to 25 A. Surprisingly, this quantity does not depend on the current I, whereas it involves the simultaneous application of both fields.

The data points are well fitted by a third-order odd polynomial in V (i.e. the sum of a term in V and a term in V^3). The fact that this effect is odd with V suggests a role of contact potentials but we have verified that the order of magnitude of $\mathcal{M}_I(\Delta_V\varphi_{EB})$ is not in agreement with other pieces of information which proves the very small influence of contact potentials. We presently have no explanation for this observation, which is still under investigation. Fortunately, the fact that this phase shift is independent of I provides a simple way of eliminating it from the HMW measurement.

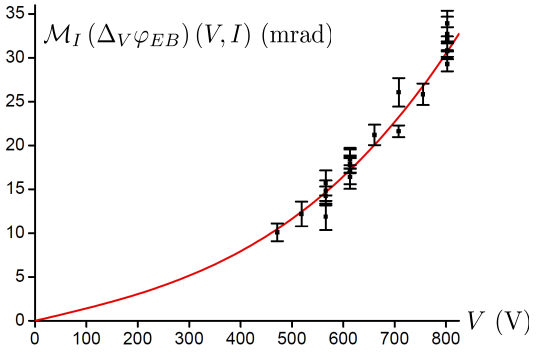

FIG. 7: The phase shift combination $\mathcal{M}_I(\Delta_V\varphi_{EB})(V, I)$ is plotted as a function of the applied voltage V. The full line is a fit with an odd polynomial in V up to third order.

VII. DETECTION OF THE HMW PHASE SHIFT

To detect the HMW phase, we may use the fact that it is odd with respect to V-reversal and I-reversal. Moreover, we must reject the largest possible part of the stray phase shifts. These ideas have led to study the difference $\varphi_{final}(V, I) = [\varphi_{EB}(V, I) - \varphi_{EB}(V, -I)]/2$: in this way, the largest stray phase shifts predicted by our model and also the I-independent unpredicted stray phase shift are both eliminated, because these two terms are both even with respect to I-reversal.

In our letter, we have plotted only the data with $|I| \leq 12$ A because the stray phase shifts increase rapidly for larger currents and the data was corrected for the AC contribution to the phase shift. In figure 8, we present all the collected data without any correction for the contribution of the AC phase shift. We have used different symbols to distinguish the measurements done with $|I| \leq 12$ or > 12A and we have made separate fits of these two sets of data using $\varphi_{final}(V, I) = \alpha VI + \beta$. The fit results are:

$$\begin{aligned} \alpha &= (-194 \pm 6) \times 10^{-8} \text{ rad/VA} \\ \beta &= (7 \pm 4) \times 10^{-4} \text{ rad} \\ \text{if} &\quad |I| \leq 12 \text{ A} \end{aligned} \tag{12}$$

and

$$\begin{aligned} \alpha &= (-216 \pm 14) \times 10^{-8} \text{ rad/VA} \\ \beta &= (-26 \pm 19) \times 10^{-4} \text{ rad} \\ \text{if} &\quad |I| > 12 \text{ A} \end{aligned} \tag{13}$$

In both fits, the intercept β for $VI = 0$ is compatible with a vanishing value, as expected. The data with $|I| \leq 12$ A is less dispersed than the data with $|I| > 12$ A and this appears clearly on the error bar of the slope α. From the spatial dependence of the magnetic and electric fields

and lithium atom electric polarizability [12], we have predicted the value of the slope of the HMW phase as a function of VI product, $\varphi_{HMW}(V,I)/(VI) = -128 \times 10^{-8}$ rad/VA. The modulus of the fitted slope is larger than the predicted value for the two fits and the discrepancy is equal 52% if $|I| \leqslant 12$ A and 69% if $|I| > 12$ A. We think that some residual stray phase shift has not been completely eliminated and the resulting error increases with the modulus of the current $|I|$. As a consequence, we consider that, even for the data set with $|I| \leqslant 12$ A, the discrepancy between the expected slope and the measured slope of φ_{final} vs VI is still dominated by this residual systematic effect.

In φ_{final}, there is a minor contribution of the AC phase shift which can be calculated thanks to our model with no adjustable parameter. We have calculated this correction which never exceeds 3 mrad for the data set with $|I| \leqslant 12$ A and we have made this correction in figure 3 of our letter. This last correction reduces the discrepancy on the slope of the measured phase φ_{final} vs. VI to 31%.

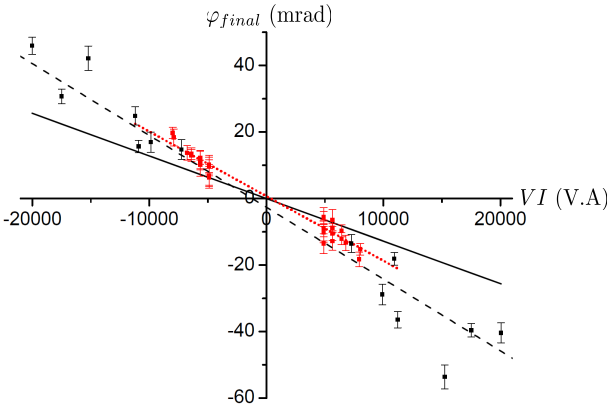

FIG. 8: Measured values of φ_{final} as a function of the VI product. The data points with $|I| \leq 12$ A are plotted in red as well as their fit represented by a dotted line. The data points with $|I| > 12$ A are plotted in black as well as their fit represented by a dashed line. The expected dependence of φ_{HMW} with VI is represented by a black full line.

VIII. CONCLUDING REMARKS

The analysis briefly summarized here explains how we have proceeded to extract the HMW phase shift from stray phase shifts due to defects of the interaction region. Indeed, thanks to its odd parity with respect to V-reversal and I-reversal, we have been able to distinguish this phase shift from various systematic effects which have been observed and fairly well explained. The description of these systematic effects is rather complex because several defects must be taken into account and also because the signal is a weighted average over 8 sub-levels. The analytical model we have developed to describe systematic effects on φ_{EB} and $\mathcal{V}_{EB}$ explains our observations in a consistent way but, in its present form, this model is not sufficient to give very accurate values of the systematic phase shifts which would be needed to extract precisely the HMW contribution to the observed phase. We attribute the discrepancy between the measured slope of φ_{final} vs VI and the expected slope of φ_{HMW} as due to residual systematic effects.

In conclusion, thanks to a thorough analysis of systematic effects, we have been able to detect the HMW phase shift but it is difficult to estimate the systematic part of our error bar. We think that it would be interesting to make a more precise measurement but this will be possible only if we are able to reduce systematic effects. The first mean will be to use smaller values of the HMW current I so that the description of the Zeeman phase shifts will be more accurate, but the most efficient technique is to eliminate the average over the 8 sub-levels which is the main source of systematic errors. Atomic beams pumped in a single sub-level with a high purity (typically more than 97% of the population can be in the selected state) have been achieved with sodium [22] and cesium [23] and we think that it should be possible to achieve a similar result with lithium. It is possible to pump the atoms either in any one of the two $m_F = 0$ sub-levels or in the $F = 2, m_F = +2$ or -2 sub-levels. The Zeeman effect of the $F = 2, m_F = +2$ or -2 sub-levels is purely linear and we think that these levels would be a better choice than the $m_F = 0$ sub-level which have a non-zero field-dependent magnetic moment as soon as hyperfine uncoupling is not negligible. With an optically pumped beam in the $F = 2, m_F = +2$ or -2 sub-level, the measurement will give the sum of the HMW and AC phase and we can separate the two contributions by changing the sign of m_F, thus changing the sign of the AC phase without changing the HMW phase.

It will be also very interesting to verify that the HMW phase is independent of the atom velocity. In our experiment, it is possible to vary the lithium beam mean velocity by changing the carrier gas, from 700 m/s (with krypton) up to 3400 m/s (helium) [24] but the distance between interferometer arms, which varies like $1/v$, becomes too small to introduce a septum when $v \gtrsim 2000$ m/s, if we use first-order diffraction. We can run the interferometer with second-order diffraction but the presence of weak first-order diffraction beams makes the experiment less clean and limits the quality of the phase measurements. With a velocity range from $700 - 2000$ m/s, a test of the variation of the HMW phase with velocity would be possible and significant if the error bar on the HMW phase is reduced near 10%.

[1] Y. Aharonov and A. Casher, Phys. Rev. Lett. **53**, 319 (1984).
[2] X.-G. He and B.H.J. McKellar, Phys. Rev. A **47**, 3424 (1993).
[3] M. Wilkens, Phys. Rev. Lett. **72**, 5 (1994).
[4] K.A. Milton Rep. Prog. Phys. **69**, 16371711(2006).
[5] H. Wei, R. Han and X. Wei, Phys. Rev. Lett. **75**, 2071 (1995).
[6] Y. Sato and R. Packard, J. Phys. Conf. Series **150**, 032093 (2009).
[7] R.C. Casella, Phys. Rev. Lett. **65**, 2217 (1990) and references therein.
[8] K. Sangster *et al.*, Phys. Rev. Lett. **71**, 3641 (1993).
[9] J.P. Dowling *et al.*, Phys. Rev. Lett. **83**, 2486 (1999).
[10] C.R. Ekstrom *et al.*, Phys. Rev. A **51**, 3883 (1995).
[11] S. Lepoutre, PhD thesis, Université P. Sabatier (2011), available on http://tel.archives-ouvertes.fr/
[12] A. Miffre *et al.*, Eur. Phys. J. D **38**, 353 (2006).
[13] P. Storey *et al.*, Journal de Physique II **4**, 1999 (1994).
[14] J. Schmiedmayer *et al.*, J. Phys. II, France **4**, 2029 (1994)
[15] D. M. Giltner, Ph. D. thesis, University of Colorado at Fort Collins (1996), unpublished.
[16] M. Jacquey *et al.*, Europhysics. Lett. (EPL) **77**, 20007 (2007).
[17] M.V. Berry (Proc. R. Soc. Lond. A **392**, 45-57 (1984)
[18] K. Abdullah *et al.*, Phys. Rev. Lett. **65**, 2347 (1990).
[19] A. Miffre, PhD thesis, Université P. Sabatier (2005), available on http://tel.archives-ouvertes.fr/
[20] C. Champenois, *et al.*, Eur. Phys. J. D **5**, 363 (1999).
[21] A. Miffre *et al.*, Eur. Phys. J. D **3**3, 99 (2005).
[22] G.W. Schinn, X.L. Han and A. Gallagher, J. Opt. Soc. Am. B **8**, 169 (1991).
[23] B.P. Masterson, C. Tanner, H. Patrick and C.E. WIemann, Phys. Rev. A **47**, 2139 (1993).
[24] S. Lepoutre *et al.*, Eur. Phys. J. D **62**, 309-325 (2011).